Effect of the deposition conditions of NiO anode buffer layers inorganic solar cells, on the properties of these cells

Duc Nguyen, A Ferrec, J Keraudy, Christian Bernède, Nicolas Stephant, Linda Cattin, P y Jouan

Applied Surface Science 311 (2014) 110–116

Contents lists available at ScienceDirect

Applied Surface Science

journal homepage: www.elsevier.com/locate/apsusc

Effect of the deposition conditions of NiO anode buffer layers in organic solar cells, on the properties of these cells

D.T. Nguyen [a], A. Ferrec [a], J. Keraudy [a,c], J.C. Bernède [b], N. Stephant [a], L. Cattin [a], P.-Y. Jouan [a,*]

[a] Institut des Matériaux Jean Rouxel (IMN), UMR 6502, Université de Nantes, 2 rue de la Houssinière, BP 92208, Nantes 44000, France
[b] MOLTECH Anjou, UMR 6200, Université de Nantes, 2 rue de la Houssinière, BP 92208, Nantes 44000, France
[c] IRT Jules Verne, Chemin du Chaffault, 44340 Bouguenais, France

ARTICLE INFO

Article history:
Received 3 September 2013
Received in revised form 4 April 2014
Accepted 5 May 2014
Available online 27 May 2014

Keywords:
Organic photovoltaic cells
Anode buffer layer
NiO thin films
DC reactive sputtering
Forming process
Annealing

ABSTRACT

NiO thin films deposited by DC reactive sputtering were used as anode buffer layer in organic photovoltaic cells (OPVs) based on CuPc/C_{60} planar heterojunctions. Firstly we show that the properties of the NiO films depend on the O_2 partial pressure during deposition. The films are first conductive between 0 and 2% partial oxygen pressure, then they are semiconductor and p-type between 2 and 6% partial oxygen pressure, between 6 and 9% partial oxygen pressure the conduction is very low and the films seem to be n-type and finally, for a partial oxygen pressure higher than 9%, the conduction is p-type. The morphology of these films depends also on the O_2 partial pressure. When the NiO films is thick of 4 nm, its peak to valley roughness is 6 nm, when it is sputtered with a gas containing 7.4% of oxygen, while it is more than double, 13.5 nm, when the partial pressure of oxygen is 16.67%. This roughness implies that a forming process, i.e. a decrease of the leakage current, is necessary for the OPVs. The forming process is not necessary if the NiO ABL is thick of 20 nm. In that case it is shown that optimum conversion efficiency is achieved with NiO ABL annealed 10 min at 400 °C.

1. Introduction

Whatever the organic photovoltaic cell (OPV) families, that based on bulk heterojunctions (BHJ) or that based on a planar heterojunction (PHJ), the carrier collection depends on the contact between the organic materials and the electrodes, the heterojunction being based on the contact between an electron donor (ED) and an electron acceptor (EA). One of the most important requirements for high power conversion efficiency of the organic solar cells is the carrier extraction from the organic diode into the electrodes. The energy barrier for hole extraction depends on the energy level difference between the work function of the electrode and the highest occupied molecular orbital (HOMO) of the organic electron donor ED. Good band matching between the anode and the ED is necessary to achieve good device performance. However the most successful anode, the indium tin oxide (ITO) has difficulties to extract holes from the ED, because of its low work function relative to the HOMO of the ED. To solve the energy level mismatch, electrodes modification is necessary [1]. One of the possibilities is the introduction of an anode buffer layer (ABL) between the ITO anode and the organic ED. One successful demonstration is using a PEDOT:PSS layer (poly(ethylenedioxythiophene):polystyrene sulphonate) [2]. However, PEDOT:PSS has been reported to present some disadvantages such as inconsistent film morphology, inefficient electron-blocking performance, poor stability under ambient conditions and it is corrosive to ITO [3]. Therefore ABL have been shown to be successful such as an ultra thin gold film [4] or a transition metal oxide [5–8]. Among the transition metal oxide, NiO has been used with success [9–13]. It has been reported that NiO thin films is a p-type semiconductor which have its valence band edge at 5.4 eV and a conduction band edge at 1.8 eV [10], so that a better energy level alignment is obtained than with ITO alone. In the present work we show that the effect of the NiO ABL on the behaviour of the organic solar cells depends strongly on the deposition conditions of NiO. As a mater of fact, the NiO films being deposited by sputtering, their properties depend strongly on the deposition conditions

2. Experimental

2.1. Anode preparation

The ITO coated glass substrates used in this study were commercially obtained from the SOLEMS. Its thickness is 100 nm, its

* Corresponding author.
E-mail address: pierre-yves.jouan@cnrs-imn.fr (P.-Y. Jouan).

http://dx.doi.org/10.1016/j.apsusc.2014.05.020
0169-4332/

conductivity is around 25 Ω/sq, its averaged transmittance in the visible is 93%, its room square means surface is 0.8 nm while its surface work function is 4.7 eV [14]. After scrubbing with soap, these ITO substrates were rinsed in running deionised water. Then the substrates were dried with a nitrogen flow and then loaded into a vacuum chamber where we proceed to the deposition of NiO. The NiO films were deposited by DC reactive magnetron sputtering using a pure nickel target (99.99%) and an $Ar + O_2$ gas mixture. We have used a target 2 inches (5.08 cm) in diameter. Substrates were placed at approximately 3 cm from the target. The gases argon and oxygen were introduced in the reactor by a mass flow controllers; the discharge current during deposition was 110 mA and 80 mA.

2.2. Solar cells realisation

In the present study, the planar solar cells used were based on the classical junction copper phthalocyanine (CuPc)/fullerene (C_{60}). CuPc is the electron donor and C_{60} the electron acceptor. It is known that a buffer layer, called exciton blocking layer (EBL), introduced between the electron acceptor and the cathode increases strongly the cells performances (Bathocuproine (BCP) or aluminium tris (8-hydroxyquinoline). In the present work aluminium Alq_3 has been used as EBL because it allows the lifetime of the OPVs. CuPc, C_{60} and Alq_3 have been deposited in a vacuum of 10^{-4} Pa. The thin film deposition rates and thickness were estimated *in situ* with a quartz monitor. The deposition rate and final thickness were 0.05 nm/s and 35 nm in the case of CuPc, 0.05 nm/s and 40 nm in the case of C_{60} and 0.1 and 9 nm for Alq_3. These thicknesses have been chosen after optimisation. After organic thin film deposition, the aluminium top electrodes were thermally evaporated, without breaking the vacuum, through a mask with 1 mm × 8 mm active areas. The ABL being the sputtered NiO film, the cells were typically: glass/ITO/NiO/CuPc/C60/BCP (or Alq_3)/Al.

2.3. Characterisation techniques

The thin films structures were analysed by X ray diffraction (XRD) by a Siemens D5000 diffractometer using Kα radiation from Cu ($\lambda_{K\alpha}$ = 0.15406 nm).

The optical measurements were carried out at room temperature using a Carry spectrometer. The film optical density was measured at wavelengths of 1.2–0.30 μm.

XPS measurements were performed with a Kratos Axis Ultra spectrometer using a source monochromator Al Kα (1486.6 eV). The spectra were recorded for NiO thin films deposited at different oxygen levels for samples with thickness of 20 nm. Kratos neutralise the system load was used for all analyses. Basic unit pressure is 8.10–8 Torr. High resolution spectra were obtained using 20 eV pass energy, an analysis area of ≈500 × 500 μm.

The morphology of the different structures used as anode was observed through scanning electron microscopy (SEM) with a JEOL 7600F at the "centre de microcaractérisation de l'Université de Nantes". Images in secondary (SEM) and backscattering (BEI) mode have been done. The composition of the films is determined by electron probe micro analysis (EPMA), the scanning electron microscope being equipped with a PGT X-ray microanalysis system; X-rays were detected by a germanium crystal.

Atomic Force Microscopy (AFM) images on different sites of the film were taken ex situ at atmospheric pressure and room temperature. All measurements have been performed in tapping mode (Nanowizard III, JPK Instruments). Classical cantilevers were used (Type PPP-NCHR-50, Nanosensor). The average force constant and resonance were approximately 14 N/m and 320 kHz, respectively. The cantilever was excited at its resonance frequency.

The majority carrier type has been checked by the hot probe technique. An n-type constantan wire was used as the reference sample. The electrical resistivity and Hall mobility of the films were determined by Hall effect measurements in a van der Pauw configuration.

Photovoltaic characterisation was performed with an automated I–V tester, in the dark and under sun global AM 1.5 simulated solar illumination. Performances of photovoltaic cells were measured using a calibrated solar simulator (Oriel 300 W) at 100 mW/cm^2 light intensity adjusted with a PV reference cell (0.5 cm^2 CIGS solar cell, calibrated at NREL, USA). Measurements were performed at an ambient atmosphere. All devices were illuminated through TCO electrodes.

3. Experimental results

3.1. Effect of the oxygen partial pressure on the properties of the NiO sputtered thin films

As described in a previous paper with a 1.3 inches target [15], there are three basic feedback signals for controlling the reactive process during sputter deposition: mass spectrometry [16], optical emission spectroscopy [17] and cathode voltage (i.e. discharge voltage) [18], which depends strongly on the properties of the material which is formed on the cathode surface during the sputtering process [19]. With a 2 inches target, we have found the same behaviour of the cathode voltage (Fig. 1) increasing the oxygen content with fixed values of current and flow of inert gas (10 sccm, standard cubic centimetre per minute, of Argon). The partial oxygen pressure has been determined by the Eq. (1).

$$\%O_2 = \frac{O_2\ \text{flux}}{O_2\ \text{flux} + \text{arflux}} \times 100 \quad (1)$$

As observed by Pierson and Rousselot for silver oxide films [20], each region exhibits a typical X-ray diffraction pattern from 1 1 1 to 2 0 0 preferential orientation through typical powder like X-ray diffraction pattern for stoichiometric films [15] and also a typical electronic behaviour. Between 0 and 2% oxygen partial pressure, the

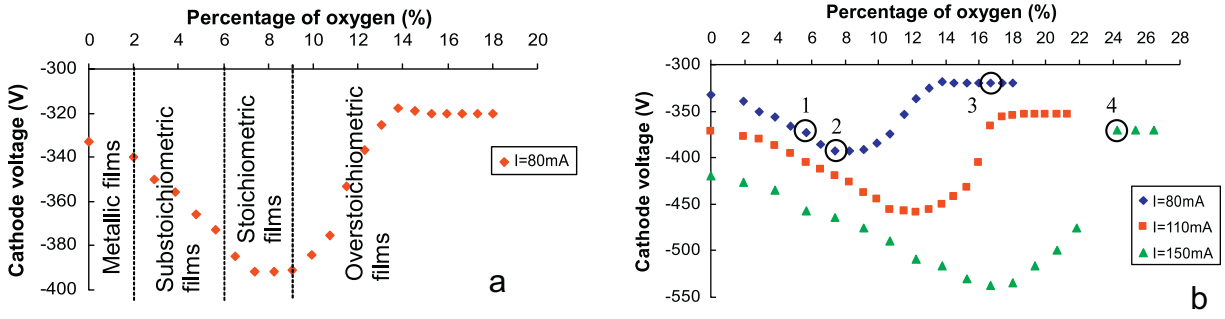

Fig. 1. (a) Different zones as a function of oxygen content, (b) voltage curves $V = f(\%O2)$ for I = 80, 110 and 150 mA.

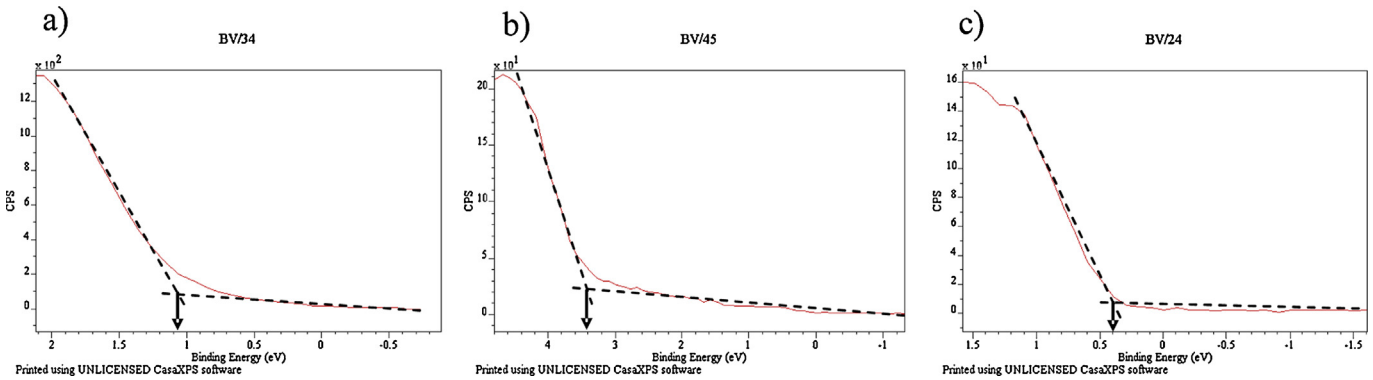

Fig. 2. XPS determination of the Fermi level EF of NiO films deposited with a discharge current of 80 mA and a partial oxygen pressure of: (a) of 5.66% O2 (point 1 in the Fig. 1); (b) of 7.4% O2 (point 2 in the Fig. 1); (c) of 16.67% O2 (point 3 in the Fig. 1).

films are conductive (metallic films). Between 2 and 6% oxygen partial pressure, the films are substoichiometric, there is O^{2-} vacancies and to maintain the electroneutrality, there is some metallic nickel. Indeed, a mixture between metallic nickel and NiO is easily formed at low oxygen ambients [21]. Therefore, metallic nickel defects and nickel vacancies coexist in a NiO film grown at low oxygen partial pressure and, as we increase oxygen content in the gas mixture, metallic nickel defects decrease and nickel vacancies increase [22].

Between 6 and 9% partial oxygen pressure the film composition is close to the stoichiometry, the conduction is very low.

Finally, for partial oxygen pressure higher than 9%, the nickel vacancies increases and Ni^{2+} is substituted by Ni^{3+} in order to maintain the electroneutrality. Typically, for $Ni_{0.95}O$ the concentration of nickel vacancies is about $6.75 \times 10^{20}/cm^3$, which would make it a highly doped p-type semiconductor [22].

As shown on Fig. 1, these four regimes depend on the discharge current (i.e.: Ni sputtered species or Ni/O ratio).

These results are comforted by the measurement of the difference between the valence band maxima (E_V) and the Fermi level (E_F) by XPS. The bind energy equal to zero corresponds to the Fermi energy which is the reference for potential if we consider that we have a good thermodynamical contact between the sample and the spectrometer. Actually the results of this difference for the zones 1, 2 and 3 are presented in Fig. 2.

For the zone 1 (5.66% O_2), $E_V - E_F = 1.1$ eV, the films are p-type. In the zone 2 (7.4% O_2), on one hand, the films have a very low conductivity (one or two order of magnitudes lower than for p-type thin films), on the other hand, $E_V - E_F = 3.5$ eV. That is the reason why we think that the films could be n-type and the band gap higher than 4 eV. Finally, in the zone 3 (16.67% O_2) $E_V - E_F = 0.4$ eV, the films are clearly p-type. These results, added to ones published in a previous paper [15], prove that all characteristics of NiO thin films such as transmittance, conduction, band gap ..., can be adjusted with plasma parameters, especially with the oxygen content in the films.

After the determination of the majority carriers of the NiO films deposited under different typical partial oxygen pressure, these NiO films were studied by AFM and SEM characterisation. Typical examples of films obtained in the sputtering conditions of zones 2 and 3 are visualised in Fig. 3 by AFM and by SEM in Fig. 4.

About the NiO thin films characterisation by AFM and by SEM, it must be highlighted that the morphology of the NiO sputtered films depends on the oxygen partial pressure. For instance, when the NiO films is thick of 4 nm, its peak to valley roughness is 6 nm, when it is sputtered with a gas containing 7.4% (zone 2, n-type) of oxygen, while it is more than double, 13.5 nm, when the partial pressure of oxygen is 16.67% (Fig. 3). These high peaks distributed all over the surface of the anode structure, can be correlated to the dark points visible in the images obtained in the backscattering mode of the SEM (Fig. 4b). Actually, the density of "black points" visible in the backscattering mode, is similar to that of the peaks visualised in the AFM images. In order to investigate the origin of these black points, we have proceeded to microprobe mapping of the visualised surfaces. Unfortunately, Ni, In and O maps are homogeneous without any features similar to that visualised by the SEM, maybe they are too small to be visualised by this technique which resolution is limited by the effect of the pear shaped interaction volume. The peak visualised by the AFM being very sharp, they may induce an effect of blindness when they are studied by SEM in the backscattering mode. Indeed, backscattered electrons leave the sample perpendicularly to its surface. Therefore, if the peaks are very sharp, they will appear black in the photos, the detector being unable to detect electron parallel to the surface of the sample.

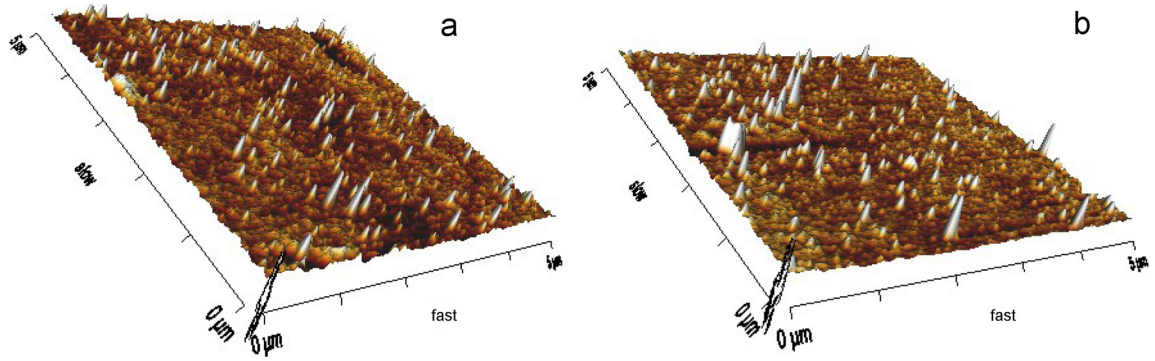

Fig. 3. AFM images of NiO films thick of 4 nm deposited in the following conditions: (a) partial oxygen pressure 7.4% O2; (b) partial oxygen pressure 16.67% O2.

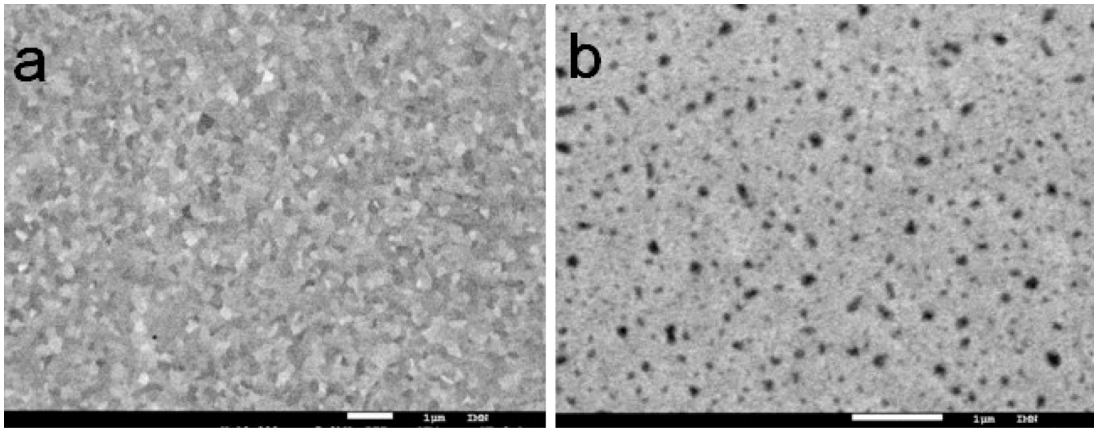

Fig. 4. Microphotographs of NiO films thick of 4 nm deposited in the following conditions: (a) partial oxygen pressure 7.4% O2 (p-type, zone 1); (b) partial oxygen pressure 16.67% O2 (p-type, zone 3).

It is known that the surface roughness of the electrode can influence the efficiency of the organic cells. As a matter of fact, a rough surface can induce a large interface between the ED and the EA, which can improve the efficiency of charge separation and therefore the Current of the OPVs. On the other hand a too high roughness of the bottom electrode may induce leakage current in the device, which decreases the shunt resistance of the diode and therefore the performance of the OPVs is poor [23]. So, since the morphology of the NiO film can be managed through the deposition conditions used, we have systematically used NiO films deposited at different O_2 partial pressure to probe the effect of the morphology of the bottom layer on the OPVs characteristics. As we can see in the next paragraph, we have also studied the influence of the thickness and the post-deposition annealing of the NiO films on the performances of the OPVs.

3.2. Organic solar cells characterisation

Firstly we have studied the influence of the O_2 partial pressure on the *J–V* characteristics of the ITO/NiO/CuPc/C60/Alq_3/Al OPVs. Typical characteristics are shown in Fig. 5 (7% O_2, NiO n-type) and Fig. 6 (16.7% O_2, NiO p-type) the NiO film being thick of 4 nm. It can be seen that there is an improvement of the OPVs performances with time during the first minutes of light exposure in the case of p-type NiO. There is something like a "forming process" for each cycle,

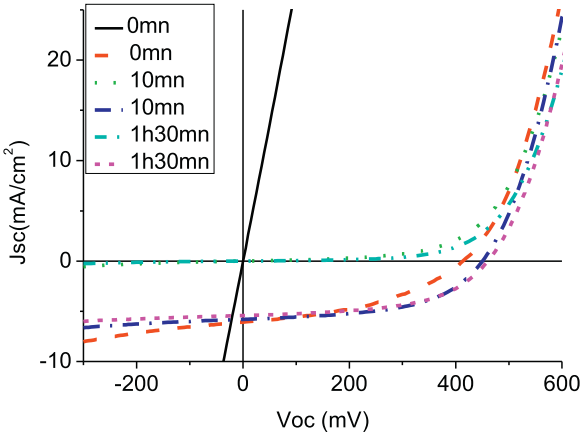

Fig. 5. The *J–V* characteristics of the cells with a NiO ABL deposited in the following conditions: 80 mA of current, 16.67% O2 and 4 nm of thickness. The different cycles were measured after a continuous exposure to AM1.5 light sources 0 min (----), 10 min (-.-.-.-) and 1 h 30 min (•••••).

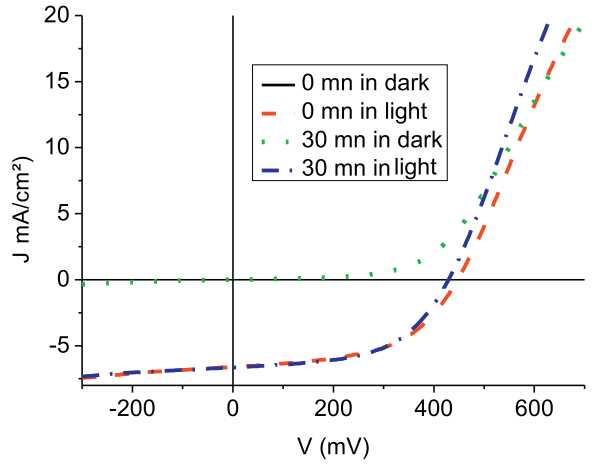

Fig. 6. The *J–V* characteristics of the cells with a NiO ABL deposited in the following conditions: 80 mA of current, 7.4% O2 and 4 nm of thickness. The different cycles were measured after a continuous exposure to AM1.5 light sources 0 min (----) and 30 min (-.-.-.-).

which consists in a decrease of the leakage current of the diode. In the dark, for the first cycle the current is ohmic. Under light there is a commutation form this ohmic behaviour to a rectifying effect. Then, the shunt resistance increase for each cycle and it stabilises after 10 of exposure to light (AM 1.5), the PCE increases from 1.48% to 1.70% (Fig. 5, Table 1). It must be noted that if the forming process, i.e. the increase of the shunt resistance, is faster under light, it is also active in the dark. In Fig. 7 one can see that there is a slow transition from the ohmic to the rectifying behaviour cycle after cycle, the measure being done in the dark. In the same way, when the measures are made under light, it can be seen in Fig. 8 that when the samples are stored in the dark between each measure, the formation of the OPVs

Table 1
Forming process under light of OPVs with NiO ABL thin films thick of 4 nm, the OPVs being submitted to continuous exposure to light.

t (min)	Voc (V)	Jsc (mA/cm²)	FF (%)	η (%)	Rs (Ω)	Rsh (Ω)
NiO, p-type, 4 nm (Fig. 5)						
0	0.460	6.21	55	1.48	3	185
10	0.470	6.16	58	1.70	3	620
300	0.490	5.84	58	1.67	4	755
NiO, n-type, 4 nm (Fig. 6)						
0	0.45	6.6	53	1.56	9	500
30	0.43	6.7	54	1.55	13	475

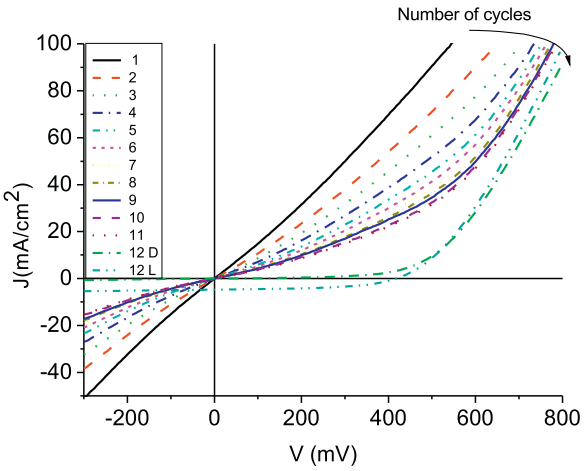

Fig. 7. The *J–V* characteristics of the cells with a NiO ABL deposited in the following conditions: 80 mA of current, 16.67% O2 and 4 nm of thickness. The sample is submitted to electrical cycles in the obscurity (11 times) and then, 1 h after, the sample is submitted to a new cycle in the obscurity and under AM1.5.

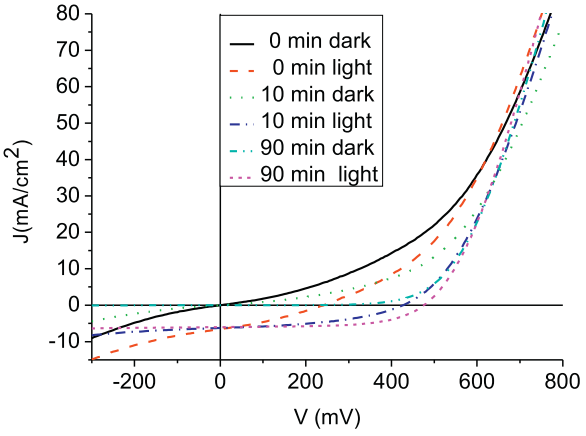

Fig. 8. The *J–V* characteristics of the cells with a NiO ABL deposited in the following conditions: 80 mA of current, 16.67% O2 and 4 nm of thickness. The different cycles were measured after 0 min (____), 10 min (-.-.-.-) and 90 min under AM1.5. After each measurement, the OPVs were placed in closed box, in the obscurity at room temperature.

is more progressive, but the stabilised efficiency is slightly higher than that obtained after continuous illumination (Table 2). In the case of n-type NiO there is no forming process (Fig. 6, Table 1), the PCE is 1.55%.

If forming processes have already been described in organic light emitting diodes (OLEDs) [24] it is not the case for OPVs. As a mater of fact, in the case of OLEDs, before the current threshold voltage, i.e. the voltage from which the current increases steeply, there are reversible micro switch effects [25]. These negative differential resistance (NDR) effects induce current change by several orders of magnitude. Such NDR are usually attributed to small short circuit effect induced by the surface roughness. It turns out that the probability for appearance of NDR decreases markedly with increasing

Table 2
The different cycles were measured after 0 min, 10 min and 1 h 30 min under AM1.5. After each measurement, the samples were placed in closed box, in the obscurity at room temperature (Fig. 8).

t (min)	Voc (V)	Jsc (mA/cm^2)	FF (%)	η (%)	Rs (Ω)	Rsh (Ω)
0	0.25	6.45	32	0.51	3.5	45
10	0.43	6.28	43	1.16	3.5	170
90	0.48	6.03	61	1.75	2.5	930

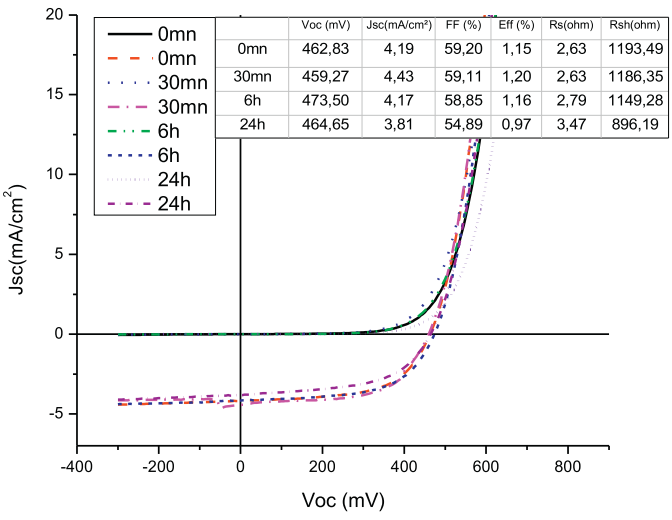

	Voc (mV)	Jsc(mA/cm²)	FF (%)	Eff (%)	Rs(ohm)	Rsh(ohm)
0mn	462,83	4,19	59,20	1,15	2,63	1193,49
30mn	459,27	4,43	59,11	1,20	2,63	1186,35
6h	473,50	4,17	58,85	1,16	2,79	1149,28
24h	464,65	3,81	54,89	0,97	3,47	896,19

Fig. 9. The *J–V* characteristics of the cells with a NiO ABL deposited in the following conditions: 150 mA of current, 23.07% O2 and 20 nm of thickness, the different cycles were measured after 0 min and 30 min, 6 h and 24 h.

thickness [26]. Such a reasoning can apply here for our cells. As a matter of fact, when it is thick of only 4 nm, the NiO film may not completely cover the ITO film. So, the difference of behaviour of the cells using a 4 nm thick NiO ABL can be related to the different morphologies of the films. When deposited under 16.67% O_2 of oxygen (p-type NiO) the peak height is more than double than that obtained with a partial pressure of 7.4 of oxygen (n-type NiO). Therefore, the vacuum deposition of organic films could be dramatically affected by "shadow effect". If the top of the anode becomes too rough, through the peaks discussed above, it would be rather difficult to cover completely uniformly the anode with the organic layer and, due to different deposition angle, the cathode can be, in very small places, in direct contact with the anode, conductive paths can form, leading to current leakage. Therefore, the ohmic like conduction of the OPVs is due to ultra thin localised metal paths bridging the top and bottom electrodes. When submitted to a potential, i.e. when a current circulates in these ultra thin filaments they are destroyed by Joule effect. Of course this effect is faster when the current is higher, which is the case when the OPVs are submitted to light. Moreover the forming process is active when NiO is p-type, that is to say when it is more conductive. It was shown, in the case of WO_3, another transition metal oxide, that, by changing the additional oxygen content of the oxide, switching insulating-conductive states may be managed. The commutation is attributed to conductive path formation [27]. When it is n-type, NiO is smooth and it is highly resistive and therefore there is not forming process.

It has already been shown that the NiO ABL improves strongly the life time of the OPVs [12], what makes possible the forming process and the improvement with time, during the first minutes of air exposure, of the PCE of the OPVs.

It is known that by modifying the thickness of the NiO ABL is possible to modify the performances of the OPVs. Therefore, in order to avoid any forming process we have increased the NiO thickness. When the NiO anode buffer layer is thick of 20 nm the *J–V* characteristics are stable as it can be seen in Figs. 9 and 10. There is no more any forming process whatever the type of the NiO, p-type or n-type (Table 3). The curves exhibit systematically a classical shape, whatever the O_2 partial pressure during NiO deposition. As a matter of fact, when the NiO film is 20 nm thick it recovers completely the ITO film, which avoids any direct contact between the anode and the cathode even if "shadow effects" are present, which

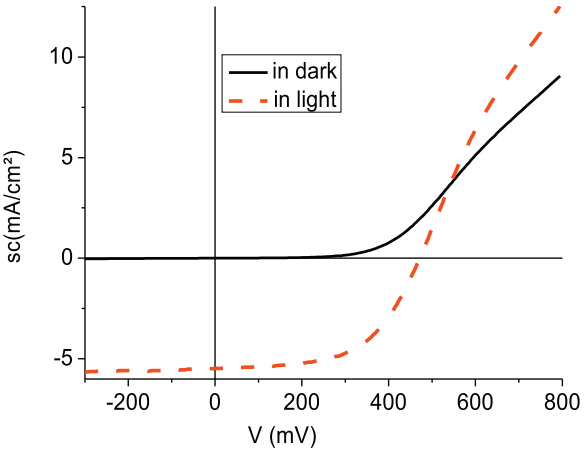

Fig. 10. The *J–V* characteristics of the cells with a NiO ABL deposited in the following conditions: 80 mA of current, 7.4% O2 and 20 nm of thickness.

Table 3
OPVs performances with NiO ABL deposited in the following conditions: 150 mA of current; 23.07%O_2 and 20 nm of thickness, the different cycles were measured after 0 min, 30 min, 6 h and 24 h.

t (min)	Voc (V)	Jsc (mA/cm^2)	FF (%)	η (%)	Rs (Ω)	Rsh (Ω)
NiO, p-type, 20 nm (Fig. 9)						
0	0.46	4.19	59	1.15	2.5	1200
30	0.46	4.43	59	1.20	2.5	1200
360	0.47	4.17	59	1.16	3	1150
1840	0.46	3.81	55	0.97	3.5	900
NiO, n-type, 20 nm (Fig. 10)						
0	0.42	5.5	56	1.5	29	1600

explains that a forming process is not necessary to achieve classical behaviour.

Therefore, in order to check the effect of annealing of the NiO ABL on the PCE of the OPVs, NiO films thick of 20 nm have been used. Before deposition of the organic layers, the ITO/NiO structures have been submitted to annealing under oxygen atmosphere for 10 min in a tubular oven. It can be seen in Fig. 11 that, up to 400 °C the annealing improves the PCE of the OPVs, for higher annealing temperature it decreases progressively (Table 4). This improvement is due to the increase of the transmittance [28].

For higher annealing temperature, the ITO bottom layer conductivity decreases, due to the decrease of oxygen vacancies and therefore the series resistance increases to the detriment of the PCE.

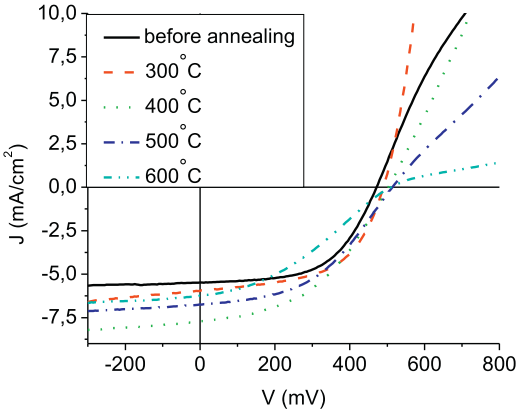

Fig. 11. The *J–V* characteristics of the cells with a NiO ABL deposited in the following conditions: 80 mA of current, 7.4% O2 and 20 nm of thickness, without annealing and after 10 min of annealing at 300 °C, 400 °C, 500 °C and 600 °C.

Table 4
Annealing effect on the performances of OPVs with NiO ABL deposited in the following conditions: 80 mA of current, 7.4%O_2 and 20 nm of thickness (Fig. 11).

Annealing temperature (°C)	Voc (V)	Jsc (mA/cm^2)	FF (%)	η (%)	Rs (Ω)	Rsh (Ω)
–	0.47	5.48	56.3	1.45	3	1600
300	0.49	5.96	55.5	1.62	3.5	500
400	0.50	7.71	45.1	1.75	21	540
500	0.51	6.75	46	1.60	47.5	710
600	0.51	6.24	35	1.11	255	560

About the thickness of the NiO ABL, it has already been shown, in the case of P3HT:PCBM bulk heterojunction that when the NiO film is thick of 4–8 nm the OPVs have poor FF, which is attributed to large leakage current and deficient electron blocking capability [11]. This result corroborates the present study, which shows that reproducible and optimum results are achieved with 20 nm thick NiO ABL.

4. Conclusions

By varying the partial oxygen pressure during NiO sputtering deposition it is possible to manage the properties of the NiO thin films. First metallic films are obtained between 0 and 2% partial oxygen pressure, then the NiO films have a p-type conduction between 2 and 6% partial oxygen pressure, between 6 and 9% partial oxygen pressure their conduction is very low and n-type. Finally, for a partial oxygen pressure higher than 9%, the conduction of the NiO films is p-type. When these films are used as ABL in ITO/NiO/CuPc/C60/BCP/Al cells the properties of these OPVs depend on the O_2 partial pressure during NiO deposition and on the thickness of this ABL. When thick of 4 nm, a forming process is present during the first electrical cycles. This forming process depends on the NiO sputtering conditions. When the films are n-type, O_2 partial pressure 7%, the forming process is marginal due to the fact that the NiO films are resistive and smooth. When the NiO films are p-type, O_2 partial pressure 16.7%, the *J–V* characteristics vary strongly during the first cycles, which is attributed to the destruction of leakage filament present in the OPVs. As a matter of fact, when deposited in these experimental conditions there is a high density of thin peaks at the surface of the NiO films and the presence of these peaks may induces ultra thin leakage filaments through some shadowing effects. The conductive filaments are destroyed by Joule effect during the forming process. In order to avoid the forming process, NiO thin films have been used as ABL. In that case optimum efficiency is achieved when the NiO is annealed at 400 °C.

References

[1] A. Godoy, L. Cattin, L. Toumi, F.R. Diaz, M.A. del Valle, G.M. Soto, B. Kouskoussa, M. Morsli, K. Benchouk, A. Khelil, J.C. Bernède, Sol. Energy Mater. Sol. Cells 94 (2010) 648.
[2] M. Cai, T. Xiao, E. Hellerich, Y. Chen, R. Shinar, J. Shinar, Adv. Mater. 23 (2011) 3590.
[3] S.-Y. Park, H.-R. Kim, H.-J. Kang, D.-H. Kim, J.-W. Kang, Sol. Energy Mater. Sol. Cells 94 (2010) 2332–2336.
[4] J.C. Bernède, L. Cattin, M. Morsli, Y. Berredjem, Sol. Energy Mater. Sol. Cells 92 (2008) 1508–1515.
[5] F. Zhang, F. Sun, Y. Shi, Z. Zhuo, L. Lu, D. Zhao, Z. Xu, Y. Wang, Energy Fuels 24 (2010) 3739.
[6] L. Cattin, F. Dahou, Y. Lare, M. Morsli, R. Tricot, S. Houari, A. Mokrani, K. Jondo, A. Khelil, K. Napo, J.C. Bernede, J. Appl. Phys. 105 (2009) 034507.
[7] M.S. Ryu, J. Jang, Sol. Energy Mater. Sol. Cells 95 (2011) 3015.
[8] I. Hancox, L.A. Rochefort, D. Clare, P. Sullivan, T.S. Jones, Appl. Phys. Lett. 99 (2011) 013304.
[9] S.-Y. Park, H.-R. Kim, Y.-J. Kang, D.-H. Kim, J.-W. Kang, Sol. Energy Mater. Sol. Cells 94 (2010) 2332.
[10] K.X. Steirer, J.P. Chesin, N.E. Widjonarko, J.J. Berry, A. Miedaner, D.S. Ginley, D.C. Olson, Org. Electron 11 (2010) 1414–1418.

[11] N. Sun, G. Fang, P. Qin, Q. Zheng, M. Wang, X. Fan, F. Cheng, J. Wan, X. Zhao, Sol. Energ. Mater. Sol. Cells 94 (2010) 2328.
[12] R. Betancur, M. Maymo, X. Elias, L.T. Vuong, J. Martorell, Sol. Energ. Mater. Sol. Cells 95 (2011) 735.
[13] M.D. Irwin, J.D. Servaites, D.B. Buchholz, B.J. Leever, J. Liu, J.D. Emery, M. Zhang, J.-H. Song, M.F. Durstock, A.J. Freeman, M.J. Bedzyk, M.C. Hersam, R.P.H. Chang, M.A. Ratner, T.J. Marks, Chem. Mater. 23 (2011) 2218.
[14] J.C. Bernède, S. Houari, D.T. Nguyen, P.Y. Jouan, A. Khelil, A. Mokrani, L. Cattin, P. Predeep, Phys. Stat. Sol. 209 (7) (2012) 1291–1297.
[15] A. Karpinski, A. Ferrec, M. Richard-Plouet, L. Cattin, M.A. Djouadi, L. Brohan, P.-Y. Jouan, Thin Solid Films 520 (2012) 3609–3613.
[16] V. Vancoppenolle, P.-Y. Jouan, M. Wautelet, J.-P. Dauchot, M. Hecq, J. Vac. Sci. Technol. A 17 (1999) 3317.
[17] V. Vancoppenolle, P.-Y. Jouan, A. Ricard, M. Wautelet, J.-P. Dauchot, M. Hecq, Appl. Surf. Sci. 205 (2003) 249.
[18] W.D. Sproul, D.J. Christie, D.C. Carter, Thin Solid Films 491 (2005) 1.
[19] D. Depla, S. Mahieu, R. De Gryse, Thin Solid Films 517 (2009) 2825.
[20] J.F. Pierson, C. Rousselot, Surf. Coat. Technol. 200 (2005) 276.
[21] S. Stanescu, C. Boeglin, A. Barbier, J.-P. Deville, Phys. Rev. B (2003), 67,035419.
[22] S. Seo, M.J. Lee, D.H. Seo, E.J. Jeoung, D.-S. Suh, Y.S. Joung, I.K. Yoo, I.R. Hwang, S.H. Kim, I.S. Byun, J.-S. Kim, J.S. Choi, B.H. Park, Appl. Phys. Lett. 85 (23) (2004).
[23] F.Z. Dahou, L. Cattin, J. Garnier, J. Ouerfelli, M. Morsli, G. Louarn, A. Bouteville, A. Khellil, J.C. Bernède, Thin Solid Films 518 (2010) 6117.
[24] J.C. Bernède, V. Jousseaume, M.A. del Valle, F.R. Diaz, Curr. Trends Polym. Sci. 6 (2001) 135.
[25] F. Brovelli, F.R. Diaz, M.A. Del Valle, J.C. Bernède, P. Molinié, Synth. Met. 122 (2000) 123.
[26] S. Berleb, W. Brütting, M. Schowoever, Synth. Met. 102 (1999) 1034.
[27] B.U. Jang, A.I. Inamdar, J. Kim, W. Jung, H. Im, H. Kim, J.P. Hong, Thin Solid Films 520 (2012) 5451.
[28] Lei Ai, Guojia Fang, Longyan Yuan, Nishuang Liu, Mingjun Wang, Chun Li, Qilin Zhang, Jun Li, Xingzhong Zhao, Appl. Surf. Sci. 254 (2008) 2401.